

The mean tilt of sunspot bipolar regions: theory, simulations and comparison with observations

N. Kleeorin,^{1,2} N. Safiullin,³ K. Kuzanyan,⁴ I. Rogachevskii,^{1,2} A. Tlatov,⁵ S. Porshnev^{3,6}

¹ Department of Mechanical Engineering, Ben-Gurion University of Negev, POB 653, 84105 Beer-Sheva, Israel

² Nordita, KTH Royal Institute of Technology and Stockholm University, Roslagstullsbacken 23, SE-10691 Stockholm, Sweden

³ Department of Radio Electronic and Informational Technology, Ural Federal University, 19 Mira str., 620002 Ekaterinburg, Russia

⁴ IZMIRAN, Troitsk, Moscow Region 108840, Russia

⁵ Kislovodsk Mountain Astronomical Station of Pulkovo Observatory, Kislovodsk, Russia

⁶ N.N. Krasovskii Institute of Mathematics and Mechanics (IMM UB RAS), Ekaterinburg, Russia

21 December 2024

ABSTRACT

A theory of the mean tilt of sunspot bipolar regions (the angle between a line connecting the leading and following sunspots and the solar equator) is developed. A mechanism of formation of the mean tilt is related to the effect of Coriolis force on meso-scale motions of super-granular convection and large-scale meridional circulation. The balance between the Coriolis force and the Lorentz force (the magnetic tension) determines a contribution of the large-scale magnetic field to the mean tilt of the sunspot bipolar regions at low latitudes. In addition, the latitudinal dependence of the solar differential rotation affects the mean tilt which can explain deviations from the Joy's law for the sunspot bipolar regions at high latitudes. The obtained theoretical results and performed numerical simulations based on the nonlinear mean-field dynamo theory which takes into account conservation of the total magnetic helicity are in agreement with observational data of the mean tilt of sunspot bipolar regions over individual solar cycles 15 - 24.

Key words: Sun: dynamo – Sun: activity

1 INTRODUCTION

Origin of solar magnetic field and dynamics of solar activity are the subjects of many studies and discussions (Moffatt 1978; Parker 1979; Krause & Rädler 1980; Zeldovich et al. 1983; Rüdiger & Hollerbach 2004; Ossendrijver 2003; Brandenburg & Subramanian 2005). The solar magnetic fields are observed in the form of sunspots and active regions. One of the characteristics of the solar bipolar region is a tilt defined as the angle between a line connecting the leading and following sunspots and circles of constant latitude parallel to the solar equator plane.

According to the Joy's law the mean tilt of sunspot bipolar regions increases with the latitude (Hale et al. 1919; Howard 1991; Sivaraman et al. 1999; Pevtsov et al. 2014; McClintock et al. 2014; McClintock & Norton 2016). The reasons for the tilt of sunspot bipolar regions are caused by effect of the Coriolis force (Fisher et al. 2000), direction of the toroidal magnetic field (Babcock 1961; Norton & Gilman 2005), and kink instability (Leighton 1969; Longcope et al. 1999; Holder et al. 2004). In particular, the main effect responsible for the formation of the mean tilt of sunspot bipolar regions is related to the effect of Coriolis force on large-scale motions in super-granular turbulent

convection. The Coriolis force is proportional to $\sin \phi$, where ϕ is the latitude, so that the main dependence of the mean tilt on the latitude is expected to be proportional to $\sin \phi$.

In spite of various theoretical, numerical and observational studies related to the mean tilt (DSilva & Choudhuri 1993; Kosovichev & Stenflo 2008; Dasi-Espuig et al. 2010; McClintock & Norton 2013; Tlatov et al. 2013; Illarionov et al. 2015; Tlatov 2015; Tlatova et al. 2015), some observational features related to the mean tilt of sunspot bipolar regions are not explained. As follows from observations (Tlatova et al. 2018), the latitudinal dependence of the mean tilt of sunspot bipolar regions is more complicated than a simple dependence as $\sin \phi$. In particular, there is a non-zero mean tilt of sunspot bipolar regions at the equator where the Coriolis force vanishes. To investigate the latitudinal dependence of the mean tilt of sunspot bipolar regions and its variations in different solar cycles, Tlatova et al. (2018) used the data of the magnetic field observations of sunspots from Mount Wilson Observatory. They have found that the latitudinal dependence of the tilt varies from one solar cycle to another, and there is a systematic offset in tilt of sunspot bipolar

arXiv:2001.01932v1 [astro-ph.SR] 7 Jan 2020

regions (non-zero tilts at the equator), with negative offset for odd cycles and positive offset for even cycles.

In the present study we develop a theory of the mean tilt of sunspot bipolar regions, taking into account effects of the solar large-scale magnetic field and the solar differential rotation on the mean tilt of sunspot bipolar regions. We have demonstrated that the balance between the Coriolis force and the magnetic tension determines a contribution of the large-scale magnetic field to the mean tilt of the sunspot bipolar regions at the low latitudes. In addition, we show that the latitudinal dependence of the solar differential rotation can affect the mean tilt. The latter can explain the observed deviations from the Joy's law for the mean tilt for the sunspot bipolar regions at the higher latitudes. The obtained theoretical results and performed numerical simulations have been compared with the latitudinal dependence of the mean tilt found in observations during the last nine solar cycles.

2 THE THEORY FOR THE MEAN TILT OF SUNSPOT BIPOLAR REGIONS

We consider the boundary between the solar convective zone and the photosphere of the Sun. In the photosphere of the Sun there is no MHD turbulence as well as the dynamo action. The mean tilt of the sunspot bipolar regions is mainly determined the effect of Coriolis force on meso-scale motions of super-granular convection and large-scale meridional circulation. In the present paper we show that there two additional contributions to the mean tilt of the sunspot bipolar regions related to (i) the effect of the large-scale magnetic field to the large-scale meridional circulation and (ii) the effect of the latitudinal dependence of the solar differential rotation.

Let us start with the momentum, induction and entropy equations using anelastic approximation and neglecting small dissipation caused by the kinematic viscosity, the magnetic diffusion and the entropy diffusion:

$$\begin{aligned} \frac{\partial \mathbf{U}}{\partial t} = & -\nabla \left(\frac{P_{\text{tot}}}{\rho_0} \right) - \mathbf{g} S + \frac{1}{4\pi\rho_0} (\mathbf{B} \cdot \nabla) \mathbf{B} \\ & + \frac{\Lambda_\rho}{8\pi\rho_0} \mathbf{B}^2 + \mathbf{U} \times (2\boldsymbol{\Omega} + \mathbf{W}), \end{aligned} \quad (1)$$

$$\frac{\partial \mathbf{B}}{\partial t} = (\mathbf{B} \cdot \nabla) \mathbf{U} - (\mathbf{U} \cdot \nabla) \mathbf{B} - \mathbf{B} (\nabla \cdot \mathbf{U}), \quad (2)$$

$$\frac{\partial S}{\partial t} = -(\mathbf{U} \cdot \nabla) S - \frac{\Omega_b^2}{g} \mathbf{U} \cdot \hat{\mathbf{r}}, \quad (3)$$

$$\nabla \cdot \mathbf{U} = \Lambda_\rho \cdot \mathbf{U}, \quad (4)$$

where \mathbf{U} and \mathbf{B} are the velocity and magnetic fields, $\mathbf{W} = \nabla \times \mathbf{U}$ is the vorticity, $P_{\text{tot}} = P + \mathbf{B}^2/8\pi + \mathbf{U}^2/2$ is the total pressure, S and P are the entropy and pressure of plasma, $\Omega_b^2 = -(\mathbf{g} \cdot \nabla) S_0$, ρ_0 and S_0 are the plasma density and entropy in the basic reference state, $\Lambda_\rho = -\nabla \ln \rho_0$, \mathbf{g} is the acceleration due to the gravity, $\hat{\mathbf{r}} = \mathbf{r}/|\mathbf{r}|$ is the unit vector in the radial direction, and $\boldsymbol{\Omega}$ is the angular velocity.

2.1 Effect of the large-scale magnetic field on the mean tilt

We decompose the solution of equations (1)–(4) as the sum of the equilibrium fields (with overbars) related to the meridional circulation and perturbations related to both, super-granular motions in the convective zone and rotational motions of sunspots in the photosphere (contributed to the mean tilt of sunspot bipolar regions), i.e., $\mathbf{U} = \overline{\mathbf{U}} + \tilde{\mathbf{u}}$, $\mathbf{B} = \overline{\mathbf{B}} + \tilde{\mathbf{b}}$, $S = \overline{S} + \tilde{s}$ and $P = \overline{P} + \tilde{p}$, where $\tilde{\mathbf{u}} = \partial \boldsymbol{\xi} / \partial t + \mathbf{v}^{(c)}$ and $\mathbf{v}^{(c)}$ is the convective velocity related to the super-granular motions. Equations (1)–(4) allow us to obtain an equation for small perturbations $\boldsymbol{\xi}$ related to the rotational motions of sunspots in the photosphere as

$$\begin{aligned} \frac{\partial^2 \boldsymbol{\xi}}{\partial t^2} = & -\nabla \left(\frac{\tilde{p}_{\text{tot}}}{\rho_0} \right) - \hat{\mathbf{r}} (\boldsymbol{\xi} \cdot \hat{\mathbf{r}}) \left(\Omega_b'^2 + \Lambda_\rho^2 \overline{U}^2 \right) \\ & + 2 \left(\overline{\mathbf{U}} + \frac{\partial \boldsymbol{\xi}}{\partial t} + \mathbf{v}^{(c)} \right) \times \boldsymbol{\Omega} + (\overline{\mathbf{U}}_A \cdot \nabla)^2 \boldsymbol{\xi} \\ & + \Lambda_\rho (\overline{\mathbf{U}}_A \cdot \nabla) [\hat{\mathbf{r}} (\overline{\mathbf{U}}_A \cdot \boldsymbol{\xi}) - \overline{\mathbf{U}}_A (\boldsymbol{\xi} \cdot \hat{\mathbf{r}})], \end{aligned} \quad (5)$$

where \tilde{p}_{tot} are the perturbations of the total pressure, and $\overline{\mathbf{U}}_A = \overline{\mathbf{B}} / (4\pi\rho_0)^{1/2}$ is the Alfvén speed, $\Omega_b'^2 = \Omega_b^2 + g(\hat{\boldsymbol{\xi}} \cdot \nabla) \overline{S} / (\hat{\boldsymbol{\xi}} \cdot \hat{\mathbf{r}})$ and $\hat{\boldsymbol{\xi}} = \boldsymbol{\xi} / |\boldsymbol{\xi}|$ is the unit vector.

Let us introduce the vector $\boldsymbol{\delta}^{\text{tw}} = \nabla \times \boldsymbol{\xi}$, which is related to the perturbations of vorticity, $\tilde{\boldsymbol{w}} \equiv (\partial / \partial t) (\nabla \times \boldsymbol{\xi}) \equiv \partial \boldsymbol{\delta}^{\text{tw}} / \partial t$. This implies that the absolute value $|\boldsymbol{\delta}^{\text{tw}}| \approx |\tilde{\boldsymbol{w}}| \delta t$ characterises the small angle in which the magnetic field lines (which are associated with the sunspot bipolar regions and connected the sunspots of the opposite magnetic polarity), are twisted during the small time δt , when the perturbations of the vorticity $\tilde{\boldsymbol{w}}$ do not vanish. The direction of the vector $\boldsymbol{\delta}^{\text{tw}}$ coincides with that of the vorticity $\tilde{\boldsymbol{w}}$, and it is perpendicular to the plane of rotation. Therefore, the radial component of the vector $\boldsymbol{\delta}^{\text{tw}}$ at the boundary between the convective zone and the photosphere can characterise the tilt of the sunspot bipolar regions. On the other hand, at this boundary the magnetic field inside the sunspots is preferably directed in the radial direction.

An equation for the mean tilt at the solar surface, $\gamma \equiv \langle \boldsymbol{\delta}^{\text{tw}} \cdot \mathbf{e}_B \rangle_{\text{time}}$, is derived in Appendix A. Here we give the derived expression for the mean tilt of the sunspot bipolar regions at the surface as

$$\gamma = \frac{\tau_A^2}{2\pi} \left\langle \nabla \times \left(\left(\overline{\mathbf{U}} + \mathbf{v}^{(c)} \right) \times \boldsymbol{\Omega} \right) \right\rangle_{\text{time}} \cdot \mathbf{e}_B, \quad (6)$$

where the angular brackets $\langle \dots \rangle_{\text{time}}$ denote the averaging over the time that is larger than the maximum Alfvén time $\tau_A = L_B / \overline{U}_A$. Here $\mathbf{e}_B = \overline{\mathbf{B}} / \overline{B}$ is the unit vector along the mean large-scale magnetic field, and L_B is the length of the magnetic field line. In the derivation of equation for the mean tilt of the sunspot bipolar regions, we take into account that $|\partial \boldsymbol{\xi} / \partial t| \ll |\mathbf{v}^{(c)}|, |\overline{\mathbf{U}}|$. We also assume that the source of the tilt of the sunspot bipolar regions, $I_\gamma = 2 \left[\nabla \times \left(\left(\overline{\mathbf{U}} + \mathbf{v}^{(c)} \right) \times \boldsymbol{\Omega} \right) \right] \cdot \mathbf{e}_B$, is localized at the vicinity of the boundary between the solar convective zone and the photosphere. Calculating the source I_γ and averaging it over the time larger than the maximum Alfvén time, we arrive at the expression for the mean tilt of sunspot bipolar regions as

$$\gamma = -\delta_0 \left[\sin \phi - \cos \phi \frac{\tau_c}{R_\odot} \frac{\partial \overline{U}_r}{\partial \phi} \right], \quad (7)$$

where $\delta_0 = (1 + \tilde{C}) \tau_A^2 \Omega / (2\pi \tau_c)$, $\tau_c = H_\rho / v_r^{(c)}$ is the characteristic time associated with convective super-granular motions, R_\odot is the solar radius, and ϕ is the latitude. Here we also took into account that $\partial v_r^{(c)} / \partial r \approx -\tilde{C} v_r^{(c)} / H_\rho$ and $\langle \partial v_r^{(c)} / \partial \phi \rangle = 0$. The radial mean velocity, \bar{U}_r is estimated as

$$\bar{U}_r = \frac{C_u}{\kappa} \left(\frac{\ell_{\text{top}}^2}{R_\odot} \right) \left(\frac{\rho_{\text{bot}}}{\rho_{\text{top}}} \right) \left(\frac{u_{\text{bot}}^2}{\nu_T^{\text{top}}} \right) \left(\frac{\partial^2 \bar{B}^2}{\partial \phi^2 \bar{B}_{\text{eq}}^2} \right)_{\text{bot}}, \quad (8)$$

(see Appendix B), where ℓ_{top} is the integral scale of turbulent motions in the upper part of the convective zone, ρ_{bot} and ρ_{top} are the plasma densities in the bottom and upper parts of the convective zone, respectively, u_{bot} and ν_T^{top} are the characteristic turbulent velocity and the turbulent viscosity, respectively, in the upper part of the convective zone, and $\bar{B}_{\text{eq}} = u \sqrt{4\pi\rho}$ is the equipartition magnetic field. The parameter $\kappa \approx 0.3 - 0.4$ characterises a fraction of the large-scale radial momentum of plasma which is lost during crossing the boundary between the convective zone and photosphere. The constant C_u in equation (8) varies from 0.7 to 1 depending on the radial profile of the mean magnetic field. Substituting equation (8) in equation (7), we obtain the expression for the mean tilt of the sunspot bipolar regions as

$$\gamma = -\delta_0 \left[\sin \phi - \delta_M \cos \phi \right], \quad (9)$$

where

$$\delta_M = C_M \left(\frac{\ell_{\text{top}}}{R_\odot} \right)^2 \left(\frac{\rho_{\text{bot}}}{\rho_{\text{top}}} \right) \left(\frac{\eta_T^{\text{bot}}}{\eta_T^{\text{top}}} \right) \left(\frac{\tau_c}{\tau_{\text{bot}}} \right) \times \left(\frac{\partial^3 \bar{B}^2}{\partial \phi^3 \bar{B}_{\text{eq}}^2} \right)_{\text{bot}}, \quad (10)$$

and $\tau_{\text{bot}} = \ell_{\text{bot}} / u_{\text{bot}}$ is the characteristic turbulent time in the bottom part of the convective zone, $C_M = 3C_u / (\kappa \text{Pr}_T) \approx 10$, $\text{Pr}_T = \nu_T / \eta_T$ is the turbulent Prandtl number and η_T is the turbulent magnetic diffusion coefficient.

The parameter δ_M describes the magnetic contribution to the mean tilt of the sunspot bipolar regions. The mechanism related to the magnetic contribution to the mean tilt is as follows. The Coriolis force results in the rotational motions of sunspots in the photosphere, and the balance between the Coriolis force and the magnetic tension determines the large-scale magnetic field contribution to the mean tilt of the sunspot bipolar regions.

To estimate the mean tilt of the sunspot bipolar regions, we use the values of governing parameters taken from models of the solar convective zone (see, e.g., Baker & Temesvary (1966); Spruit (1974); more modern treatments make little difference to these estimates). In particular, at depth $H \sim 2 \times 10^{10}$ cm (i.e., at the bottom of the convective zone), the magnetic Reynolds number $\text{Rm}^{\text{bot}} = u_{\text{bot}} \ell_{\text{bot}} / \eta = 2 \cdot 10^9$ (where η is the magnetic diffusion coefficient due to electrical conductivity of plasma), the turbulent velocity $u_{\text{bot}} \sim 2 \times 10^3$ cm s⁻¹, the integral scale of turbulence $\ell_{\text{bot}} = 8 \times 10^9$ cm, the plasma density $\rho_{\text{bot}} = 2 \times 10^{-1}$ g cm⁻³, and the turbulent diffusion coefficient $\eta_T^{\text{bot}} = 5.3 \times 10^{12}$ cm² s⁻¹. The density stratification scale is estimated here as $H_\rho^{\text{bot}} = \rho / |\nabla \rho| = 6.5 \times 10^9$ cm and the equipartition mean magnetic field $\bar{B}_{\text{eq}}^{\text{bot}} = 3000$ G. In the upper part of the convective zone, say at depth $H \sim 2 \times 10^7$ cm, these

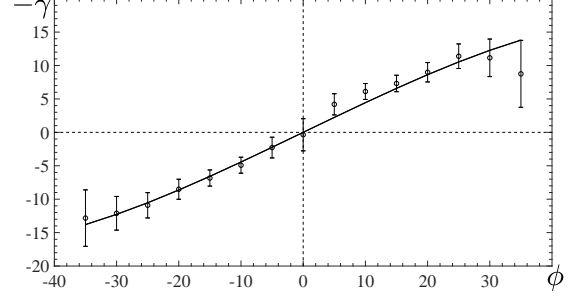


Figure 1. The mean tilt $-\gamma$ (in degrees) versus the latitude ϕ (in degrees): Eq. (12) of our theory with $\delta_0 = 0.35$, $\delta_3 = 0.12$, $\delta_5 = 1.6 \times 10^{-2}$, $\tilde{\delta}_3 = 4.48$, $\tilde{\delta}_5 = 1.02$ and $\tilde{\delta}_M = 0$ (solid line) and the data from observations (circles) of all solar cycles published in Fig. 3 of Tlatova et al. (2018).

parameters are $\text{Rm}^{\text{top}} = u_{\text{top}} \ell_{\text{top}} / \eta = 10^5$, $u_{\text{top}} = 9.4 \times 10^4$ cm s⁻¹, $\ell_{\text{top}} = 2.6 \times 10^7$ cm, $\rho_{\text{top}} = 4.5 \times 10^{-7}$ g cm⁻³, $\eta_T^{\text{top}} = 0.8 \times 10^{12}$ cm² s⁻¹, $H_\rho^{\text{top}} = 3.6 \times 10^7$ cm, and the equipartition mean magnetic field is $\bar{B}_{\text{eq}}^{\text{top}} = 220$ G.

Using these estimates, we calculate the parameters δ_0 and δ_M which determine the mean tilt of the sunspot bipolar region. Taking the Alfvén speed $\bar{U}_A = 5 \times 10^4$ cm s⁻¹, the length the magnetic field line $L_B = 4H_\rho = 4 \times 10^9$ cm, we obtain the Alfvén time $\tau_A = L_B / \bar{U}_A = 10^5$ s. Taking the convective velocity $u_c = (3 - 5) \times 10^4$ cm s⁻¹, we obtain the convective time as $\tau_c = (2 - 3) \times 10^4$ s. This yields $\delta_0 = 0.3 - 0.5$ (in radians) and $\delta_M = 0.05 - 0.2$. This implies that the magnetic contribution δ_M to the mean tilt γ is essential only in the low latitude region where $\sin \phi$ is small.

2.2 Effect of latitudinal dependence of the solar rotation on the mean tilt

In this section we take into account an effect of latitudinal dependence of the solar differential rotation on the tilt of the sunspot bipolar regions. In particular, the latitudinal dependence of the solar rotation can be approximated by

$$\Omega = \Omega_0 (1 - C_2 \sin^2 \phi - C_4 \sin^4 \phi), \quad (11)$$

[see LaBonte & Howard (1982)], where $\Omega_0 = 2.83 \times 10^{-6}$ s⁻¹, $C_2 = 0.121$ and $C_4 = 0.173$. Substituting equation (11) into equation (9) with $\delta_0 = (1 + \tilde{C}) \tau_A^2 \Omega / (2\pi \tau_c)$, we obtain

$$\gamma = -\tilde{\delta}_0 \left[\sin \phi + \delta_3 \sin 3\phi - \delta_5 \sin 5\phi - \tilde{\delta}_M \left(\cos \phi + \tilde{\delta}_3 \cos 3\phi - \tilde{\delta}_5 \cos 5\phi \right) \right], \quad (12)$$

where $\tilde{\delta}_0 = C_D \delta_0$, $\tilde{\delta}_M = \delta_M \tilde{C}_D / 16C_D$, $C_D = 1 - (3C_2 + 5C_4) / 4 \approx 0.693$, $\tilde{C}_D = 1 - 4C_2 - 2C_4 \approx 0.17$ and $\delta_3 = (4C_2 + 5C_4) / 16C_D \approx 0.122$, $\delta_5 = C_4 / 16C_D \approx 1.56 \times 10^{-2}$, $\tilde{\delta}_3 = (4C_2 + 3C_4) / \tilde{C}_D \approx 4.48$, and $\tilde{\delta}_5 = C_4 / \tilde{C}_D \approx 1.02$. For the derivation of equation (12) we take into account that $\Omega / H_\rho \gg |\partial \Omega / \partial r|$ and $\Omega / H_\rho \gg r^{-1} |\partial \Omega / \partial \theta|$, and we also use identities given in Appendix C.

In Figure 1 we show the mean tilt $-\gamma$ (solid line) versus latitude ϕ given by equation (12) of our theory, where γ and ϕ are measured in degrees, and we use the following values of parameters: $\tilde{\delta}_0 = 0.35$, $\delta_3 = 0.12$, $\delta_5 = 1.6 \times 10^{-2}$,

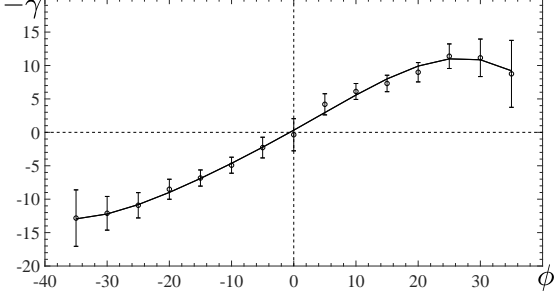


Figure 2. The mean tilt $-\gamma$ (in degrees) versus latitude ϕ (in degrees): Eq. (12) of our theory with $\tilde{\delta}_0 = 0.31$, $\tilde{\delta}_3 = 1.26$, $\tilde{\delta}_5 = 0.22$, $\tilde{\delta}_3 = 1.87$, $\tilde{\delta}_5 = 0.78$ and $\tilde{\delta}_M = 0.2$ (solid line), and the data from observations (circles) of all solar cycles published in Fig. 3 of Tlatova et al. (2018).

$\tilde{\delta}_3 = 4.48$, $\tilde{\delta}_5 = 1.02$ and $\tilde{\delta}_M = 0$ (i.e., the magnetic contribution to the mean tilt of the sunspot bipolar regions is neglected here). For comparison with observations, we also show in Figure 1 the data obtained from observations of all solar cycles presented in Figure 3 of Tlatova et al. (2018) and shown here as circles (see Section 4 for more details about the observational data). The observational data have been averaged over bipolar regions of all sizes [see Tables 1 and 2 in Tlatova et al. (2018)], where the mean value and the standard deviation of Gaussian fittings have been computed.

In Figure 2 we also show the theoretical latitudinal dependence of the mean tilt $-\gamma$ (solid line), taking into account the magnetic contribution to the mean tilt of the sunspot bipolar regions ($\tilde{\delta}_M = 0.2$). Slightly varying the values of other coefficients ($\tilde{\delta}_0 = 0.31$, $\tilde{\delta}_3 = 1.26$, $\tilde{\delta}_5 = 0.22$, $\tilde{\delta}_3 = 1.87$ and $\tilde{\delta}_5 = 0.78$), we obtain a good agreement between the theoretical predictions for the mean tilt and the observational data (see Figure 2).

3 NUMERICAL MODELLING OF THE MEAN TILT OF SUNSPOT BIPOLAR REGIONS

To obtain the time evolution of the mean tilt of sunspot bipolar regions, in particular, to get the butterfly diagram of the mean tilt, we use a nonlinear mean-field dynamo model discussed in details by Kleorin et al. (2016); Safiullin et al. (2018). This model describes the time evolution of the mean magnetic field. Below we briefly outline this model. The mean-field dynamo equations are given by:

$$\frac{\partial \overline{B}_\varphi}{\partial t} = GD \sin \theta \frac{\partial \overline{A}}{\partial \theta} + \frac{\partial^2 \overline{B}_\varphi}{\partial \theta^2} - \mu^2 \overline{B}_\varphi, \quad (13)$$

$$\frac{\partial \overline{A}}{\partial t} = \alpha \overline{B}_\varphi + \frac{\partial^2 \overline{A}}{\partial \theta^2} - \mu^2 \overline{A}, \quad (14)$$

where we use spherical coordinates (r, θ, φ) for an axisymmetric large-scale magnetic field, $\overline{\mathbf{B}} = \overline{B}_\varphi \mathbf{e}_\varphi + \nabla \times (\overline{A} \mathbf{e}_\varphi)$. We consider the mean-field dynamo in a thin convective shell, taking into account strong variation of the plasma density in the radial direction by averaging the equations for the mean toroidal field \overline{B}_φ and the magnetic potential

\overline{A} of the mean poloidal field over the depth of the convective shell. We neglect the curvature of the convective shell and replace it by a flat slab. The terms describing turbulent diffusion of the mean magnetic field in the radial direction in equations (13) and (14) in the framework of the no- z model are given as $-\mu^2 \overline{B}_\varphi$ and $-\mu^2 \overline{A}$ (Kleorin et al. 2016; Safiullin et al. 2018), and see also references therein. The differential rotation is characterised by parameter $G = \partial \Omega / \partial r$, and the parameter μ is determined by the following equation: $\int_{2/3}^1 (\partial^2 \overline{B}_\varphi / \partial r^2) dr = -(\mu^2 / 3) \overline{B}_\varphi$.

Equations (13)–(14) are written in a non-dimensional form so that the length is measured in units of the solar radius R_\odot , time is measured in units of the turbulent magnetic diffusion time R_\odot^2 / η_T , the differential rotation $\delta \Omega$ is measured in units of the maximal value of the angular velocity Ω , and α is measured in units of the maximum value of the kinetic part of the α -effect. The toroidal mean magnetic field, \overline{B}_φ is measured in the units of the equipartition field $\overline{B}_{\text{eq}} = u \sqrt{4\pi \rho_{\text{bot}}}$, and the vector potential of the mean poloidal field \overline{A} is measured in units of $R_\alpha R_\odot \overline{B}_{\text{eq}}$. The density ρ_0 is normalized by its value ρ_{bot} at the bottom of the convective zone, and the integral scale of the turbulent motions ℓ and turbulent velocity u at the scale ℓ are measured in units of their maximum values through the convective region. The magnetic Reynolds number $\text{Rm} = \ell u / \eta$ is defined using the maximal values of the integral scale ℓ and the characteristic turbulent velocity u , and the turbulent magnetic diffusion coefficient is $\eta_T = \ell u / 3$.

We use the standard profile of the kinetic part of the α effect: $\alpha(\theta) = \alpha_0 \sin^3 \theta \cos \theta$. The dynamo number is defined as $D = R_\alpha R_\omega$, where $R_\alpha = \alpha_0 R_\odot / \eta_T$ and $R_\omega = (\delta \Omega) R_\odot^2 / \eta_T$. Equations (13) and (14) describe the dynamo waves propagating from the central latitudes towards the equator when the dynamo number is negative. The radius r varies from $2/3$ to 1 inside the convective shell, so that the value $\mu = 3$ corresponds to a convective zone with a thickness of about $1/3$ of the radius.

The total α effect is defined as the sum of the kinetic and magnetic parts: $\alpha(\theta) = \chi_v \Phi_v(\overline{B}) + \sigma \chi_c \Phi_m(\overline{B})$ (Kleorin et al. 2016; Safiullin et al. 2018), where $\chi_v = -(\tau/3) \mathbf{u} \cdot (\nabla \times \mathbf{u})$, $\chi_c = (\tau/12\pi\rho) \mathbf{b} \cdot (\nabla \times \mathbf{b})$, τ is the correlation time of the turbulent velocity field, \mathbf{u} and \mathbf{b} are the velocity and magnetic fluctuations, and $\sigma = \int_{2/3}^1 (\rho_0(r) / \rho_{\text{bot}})^{-1} dr$. The magnetic part of the α effect (Frisch et al. 1975; Pouquet et al. 1976) and density of the magnetic helicity are related to the density of the current helicity $\mathbf{b} \cdot (\nabla \times \mathbf{b})$ in the approximation of weakly inhomogeneous turbulent convection (Kleorin & Rogachevskii 1999). The quenching functions $\Phi_v(\overline{B})$ and $\Phi_m(\overline{B})$ in equation for the total α effect are given by: $\Phi_v(\overline{B}) = (1/7)[4\Phi_m(\overline{B}) + 3\Phi_B(\overline{B})]$ and $\Phi_m(\overline{B}) = (3/8\overline{B}^2)[1 - \arctan(\sqrt{8\overline{B}}/\sqrt{8\overline{B}})]$ (Rogachevskii & Kleorin 2000, 2001, 2004), where $\Phi_B(\overline{B}) = 1 - 16\overline{B}^2 + 128\overline{B}^4 \ln[1 + 1/(8\overline{B}^2)]$, and χ_v and χ_c are measured in units of maximal value of the α -effect. The function Φ_v describes the algebraic quenching of the kinetic part of the α effect that is caused by the effects of the mean magnetic field on the electromotive force. The densities of the helicities and quenching functions are associated with a middle part of the convective zone. The parameter $\sigma > 1$ is a free parameter.

The magnetic part α_m of the α effect is based on

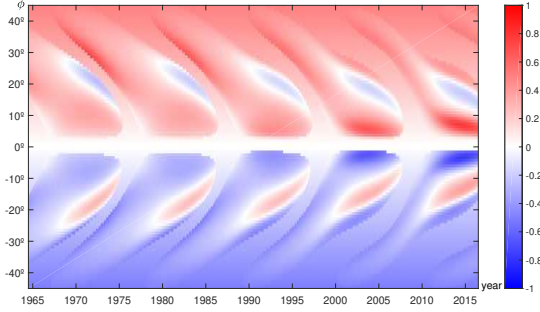


Figure 3. Butterfly diagram of the normalised mean tilt $-\gamma/\delta_0$ with the spot formation threshold, $\overline{B}_{\text{th}} = 0.4 B_0$.

two nonlinearities: the algebraic nonlinearity (quenching of α_m), given by the function $\Phi_m(\overline{B})$, and the dynamic nonlinearity. The function $\chi_c(\overline{B})$ is determined by a non-dimensional dynamical equation (Kleeorin & Ruzmaikin 1982; Kleeorin & Rogachevskii 1999; Kleeorin et al. 1995, 2000, 2002, 2003a,b; Brandenburg & Subramanian 2005; Zhang et al. 2006, 2012):

$$\begin{aligned} \frac{\partial \chi_c}{\partial t} + (\tau_\chi^{-1} + \kappa_T \mu^2) \chi_c = 2 \left(\frac{\partial \overline{A}}{\partial \theta} \frac{\partial \overline{B}_\varphi}{\partial \theta} + \mu^2 \overline{A} \overline{B}_\varphi \right) \\ - \left(\frac{R_\odot^2}{2\ell^2} \right) \alpha \overline{B}^2 - \frac{\partial}{\partial \theta} \left(\overline{B}_\varphi \frac{\partial \overline{A}}{\partial \theta} - \kappa_T \frac{\partial \chi_c}{\partial \theta} \right), \end{aligned} \quad (15)$$

where $\mathbf{F}_\chi = -\kappa_T \nabla \chi_c$ is the turbulent diffusion flux of the density of the magnetic helicity, κ_T is the coefficient of the turbulent diffusion of the magnetic helicity, $\tau_\chi = \ell^2/\eta$ is the relaxation time of magnetic helicity. This equation is derived from the conservation law for magnetic helicity. The average value of τ_χ^{-1} is given by

$$\tau_\chi^{-1} = H^{-1} \int_{2/3}^1 \tilde{\tau}_\chi^{-1}(r) dr \sim \frac{H_\ell R_\odot^2 \eta}{H \ell^2 \eta_T}, \quad (16)$$

where H is the depth of the convective zone, H_ℓ is the characteristic scale of variations ℓ , and $\tilde{\tau}_\chi(r) = (\eta_T/R_\odot^2)(\ell^2/\eta)$ is the non-dimensional relaxation time of the density of the magnetic helicity. The values H_ℓ , η , ℓ in equation (16) are associated with the upper part of the convective zone. The mean magnetic field is given by

$$\overline{B}^2 = \frac{2\ell^2}{R_\odot^2} \left[\overline{B}_\varphi^2 + R_\alpha^2 \left(\mu^2 \overline{A}^2 + \left(\frac{\partial \overline{A}}{\partial \theta} \right)^2 \right) \right]. \quad (17)$$

The solar activity is characterised by the Wolf number (Gibson 1973; Stix 1989), that is defined as $W = 10g_w + f_w$, where g_w is the number of sunspot groups and f_w is the total number of sunspots in the visible part of the sun. In the framework of the nonlinear mean-field dynamo model by Kleeorin et al. (2016); Safiullin et al. (2018), the phenomenological budget equation for the surface density of the Wolf number is given by equation (D1) in Appendix D.

We solve numerically Eqs. (13), (14), (15) and (D1). We use the following initial conditions: $\overline{B}_\varphi(t=0, \theta) = S_1 \sin \theta + S_2 \sin(2\theta)$ and $\overline{A}(t=0, \theta) = 0$. The parameters of the numerical simulation are as follows: $D = -8450$, $G = 1$, $\sigma = 3$, $\mu = 3$, $\kappa_T = 0.1$, $R_\alpha = 2$, $\tau_\chi = 6.3$, $S_1 = 0.051$ and $S_2 = 0.95$. The choice of these parameters in the numerical simulations is caused by the following reasons. In our

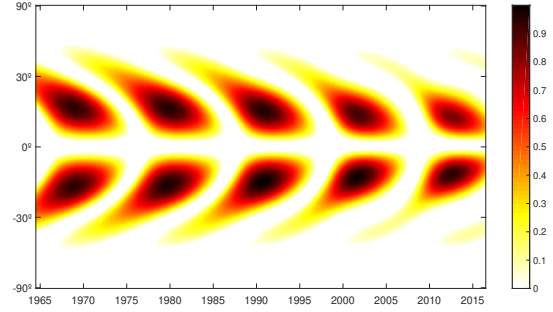


Figure 4. Butterfly diagram of the surface density of the Wolf numbers with the threshold $0.4 B_0$ for the magnetic spot formation.

previous studies (Kleeorin et al. 2016; Safiullin et al. 2018) we performed a parameter scan using about 10^3 runs with different sets of parameters to find an optimal set of parameters to reach a high level of correlation between the dynamo model results and observations of the Wolf numbers. The variations of the parameters affect the results as follows. There are two crucial parameters which strongly affect the dynamics of the nonlinear dynamo system: the dynamo number D and the initial field $B_{\text{init}}^{\text{dip}}$ for the dipole mode, determined by the parameter S_2 . A proper choice of the initial field $B_{\text{init}}^{\text{dip}}$ allows to avoid very long transient regimes.

Comparing the results of the dynamo model with observations, we determine the correlation between the numerical simulation results for the evolution of the Wolf number and the observational data. To find the maximum correlation between the dynamo model results and the observed Wolf numbers, the following parameter scan has been performed: $-8800 \leq D \leq -8200$ and $0.85 \leq S_2 \leq 0.95$ [see Fig. 12 in Kleeorin et al. (2016)]. The maximum correlation is obtained when the parameters are $D = -8450$ and $S_2 = 0.95$. The parameter μ determines the critical dynamo number, $|D_{\text{cr}}|$, for the excitation of the large-scale dynamo instability. The flux of the magnetic helicity [see Eq. (15)], characterised by the parameter κ_T , cannot be very small to avoid the catastrophic quenching of the α effect (Kleeorin et al. 2000, 2002, 2003a,b). The optimal value for this parameter is $\kappa_T \approx 0.1$. The variations of the other parameters only weakly affect the obtained results (Kleeorin et al. 2016).

Using results of these numerical simulations, we plot in Fig. 3 the butterfly diagram of the normalised mean tilt $-\gamma/\delta_0$ given by equation (9) with the magnetic contribution to the mean tilt as

$$\delta_M(\overline{B}^2) = C_* \left(\frac{\partial^3 \overline{B}^2}{\partial \phi^3 B_{\text{eq}}^2} \right)_{\text{bot}}, \quad (18)$$

$\phi = \pi/2 - \theta$ is the latitude, and the exact value of the free parameter C_* is determined to obtain good agreement with observational data on the mean tilt of sunspot bipolar regions. For comparison, in Fig. 4 we show the butterfly diagram of the surface density of the Wolf numbers using the threshold $0.4 B_0$ for the magnetic spot formation. First, the butterfly diagram of the normalised mean tilt of sunspot bipolar regions is essentially different from that of the surface density of the Wolf numbers. In particular, the mean tilt distribution in every hemisphere is nearly homogeneous,

i.e., it depends weakly on the phase of the solar cycle except for small regions for the low latitudes where the mean tilt has opposite signs in every hemisphere. On the other hand, the distribution of the surface density of the Wolf number is strongly inhomogeneous, i.e., it strongly depends on the phase of the solar cycle.

4 COMPARISON WITH OBSERVATIONS

In this section we compare our numerical results with observational data of the mean tilt $-\gamma$ of sunspot bipolar regions. We use the observational data which have been obtained by Tlatova et al. (2018) from daily sunspot drawings taken at Mount Wilson Observatory (MWO). The data cover a century long period. The original MWO drawings were digitized using software package developed by Tlatova et al. (2015), see also references therein. The digitization includes the date and time of observations, heliographic coordinates of each umbra, its area, the strength, and polarity of its magnetic field. The overall digitized dataset used by us contains the total number of 20,318 days of observations, from 1917 to October 2016. The method of Tlatova et al. (2018) enables to identify clusters of sunspots of positive and negative polarity, from which bipolar pairs have been formed.

There has been the total of 441,973 measurements of the magnetic field of individual nuclei and pores of sunspots carried out, and the total number of 51,413 bipolar regions allocated. Initially, clusters of active regions of positive and negative polarity were searched for. For achieving this, the sunspots were sorted by area for each day of observation, and kernels of the same polarity located at a distance of no more than 10 degrees in longitude and 7 degrees in latitude from the spot of maximum area were selected. For each cluster, the average coordinates were found, which were computed using the weight function over the area. Next, a bipole counterpart through clusters of sunspot negative polarity was found.

The observational data are two-fold. The first group of the data used in the present study to produce Figures 1 and 2 (see Section 2), is the result of averaging of bipolar pairs of all sizes. This group of the data is presented in Tables 1 and 2 in Tlatova et al. (2018), where the mean value and the standard deviation of Gaussian fittings have been computed. We use the data to compare with the the mean tilts computed according to our theory. We have shown that the theoretical results fit the observations very well. The data have been filtered out by the bipolar regions smaller in length than 3 degrees. In total there were 18,547 bipolar regions in the even and 17,435 in the odd solar cycles. We used the bipolar regions greater than 3 degrees because smaller bipolar regions almost do not possess a certain tilt angles.

The second group of the data used below to produce Figure 5 is comprised of the all data on the tilts of all bipolar regions filtered by the small sized bipolar pairs, so that only the bipolar regions larger by size than 3 degrees were retained. The cut-off area of those pairs was set to several μH ($4\pi \times 10^{-6}$ of steradian). We have used those data to confront with our theoretical results based on the time evolution of the mean tilt of sunspot bipolar regions computed

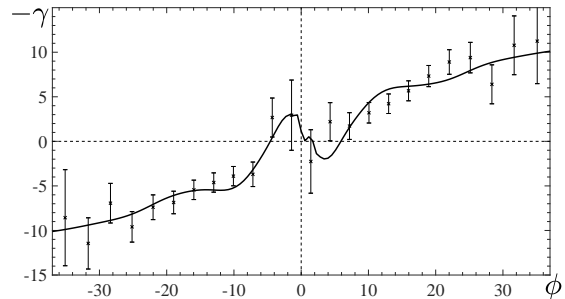


Figure 5. The mean tilt $-\gamma$ (in degrees) versus the latitude ϕ (in degrees): numerical simulations (solid line) and observations of sunspot bipolar regions (dashed line) averaged over individual cycles 15 - 24.

from dynamo models and related to the magnetic contribution to the mean tilt.

Note that both these samplings are very different from what was published for statistics of bipolar regions earlier by Tlatov et al. (2013); Tlatov (2015). In earlier works the bipolar regions have been composed from individual sunspot nuclei, while in our studies they are formed from the clusters of sunspots. Thus, our results may be qualitatively very different from those of Kosovichev & Stenflo (2008); Dasi-Espuig et al. (2010). Since the nuclei of spots are formed of the two opposite polarities, the technique and the results are significantly different.

In Figure 5 we show the mean tilt $-\gamma$ (in degrees) versus the latitude ϕ obtained in this numerical simulation (see solid line in Figure 5) for $C_* = 0.8$, $\delta_0 = 0.29$, $\delta_3 = 0.122$, $\delta_5 = 1.56 \times 10^{-2}$, $\tilde{\delta}_3 = 4.48$, and $\tilde{\delta}_5 = 1.02$. These numerical results are also compared with the observational data of the mean tilt $-\gamma$ of sunspot bipolar regions. The observational data have been averaged over individual solar cycles (from the cycle 15 to 24). The numerical results are also averaged over the same cycles. It follows from Figure 5 that there is an asymmetry between the northern and southern hemisphere. We stress that we have taken into account here an effect of the latitudinal dependence of the solar differential rotation on the mean tilt of the sunspot bipolar regions as well as the contribution to the mean tilt caused by the large-scale magnetic field. The obtained theoretical results and performed numerical simulations for the mean tilt of sunspot bipolar regions are in an agreement with the observational data.

5 CONCLUSIONS

We have developed a theory of the mean tilt of sunspot bipolar regions. The formation of the mean tilt is caused by the effect of the Coriolis force on meso-scale motions of supergranular convection and large-scale meridional circulation. We have demonstrated that at low latitudes the joint action of the Coriolis force and the magnetic tension results in an additional contribution to the mean tilt of the sunspot bipolar regions which depends on the large-scale magnetic field. We have also found an additional contribution to the mean tilt of the sunspot bipolar regions which is caused by an effect of the latitudinal dependence of the solar differential rotation on the mean tilt. The latter can explain the devia-

tions from the Joy's law for the mean tilt at high latitudes. The obtained theoretical results and performed numerical simulations for the mean tilt are in an agreement with the observational data of the mean tilt of the sunspot bipolar regions.

ACKNOWLEDGMENTS

Stimulating discussions with participants of the NORDITA program on "Solar Helicities in Theory and Observations: Implications for Space Weather and Dynamo Theory" (March 2019) are acknowledged. The work of KK and NS was supported in part by a grant from the Russian Science Foundation (grant RNF 18-12-00131) at the Crimean Astrophysical Observatory. AT would like to acknowledge support from RFBR grant 18-02-00098 for the observational data analysis. NK, KK, IR acknowledge the hospitality of NORDITA.

REFERENCES

Babcock, H. W., 1961, ApJ, 133, 572
 Baker N., Temesvary S., 1966, Tables of Convective Stellar Envelope Models, New York
 Brandenburg A., Gressel O., Jabbari S., Kleeorin N., Rogachevskii I., 2014, A&A, 562,A53
 Brandenburg A., Kemel K., Kleeorin N., Mitra D., Rogachevskii I., 2011, ApJ, 740, L50
 Brandenburg A., Kleeorin N., Rogachevskii I., 2013, ApJ, 776, L23
 Brandenburg A., Rogachevskii I., Kleeorin N., 2016, New J. Phys., 18, 125011
 Brandenburg A., Subramanian K., 2005, Phys. Rep., 417, 1
 Dasi-Espuig M., Solanki S.K., Krivova N.A., Cameron R., Peñuela T., 2010, A&A, 518, A7
 DSilva S., Choudhuri A. R., 1993, A&A, 272, 621
 Fisher G. H., Fan Y., Longcope D. W., Linton M. G., Pevtsov A. A., 2000, Solar Phys. 192, 119
 Frisch U., Pouquet, A., Leorat, I., Mazure, A. 1975, J. Fluid Mech., 68, 769
 Gibson E. G., 1973, The Quiet Sun, NASA, Washington
 Hale G. E., Ellerman F., Nicholson S. B., Joy, A. H., 1919, ApJ, 49, 153.
 Holder Z. A., Canfield R. C., McMullen R. A., Nandy D., Howard R. F., Pevtsov A. A., 2004, ApJ, 611, 1149
 Howard R. F., 1991, Solar Phys. 136, 251
 Illarionov E., Tlatov A., Sokoloff D., 2015, Solar Phys. 290, 351
 Käpylä P., Brandenburg A., Kleeorin N., Mantere M., Rogachevskii I., 2012, MNRAS, 422, 2465
 Käpylä, P. J., Brandenburg, A., Kleeorin, N., Käpylä, M. J., & Rogachevskii, I. 2016, A&A, 588, A150
 Kleeorin N., Kuzanyan K., Moss D., Rogachevskii I., Sokoloff D., Zhang H., 2003a, A&A, 409, 1097
 Kleeorin N., Mond M., Rogachevskii I., 1993, Phys. Fluids B, 5, 4128
 Kleeorin N., Mond M., Rogachevskii I., 1996, A&A, 307, 293

Kleeorin N., Moss D., Rogachevskii I., Sokoloff D., 2000, A&A, 361, L5
 Kleeorin N., Moss D., Rogachevskii I., Sokoloff D., 2002, A&A, 387, 453
 Kleeorin N., Moss D., Rogachevskii I., Sokoloff D., 2003b, A&A, 400, 9
 Kleeorin N., Rogachevskii I., 1994, Phys. Rev. E, 50, 2716
 Kleeorin N., Rogachevskii I., 1999, Phys. Rev. E, 59, 6724
 Kleeorin N., Rogachevskii I., Ruzmaikin A. A., 1989, Sov. Astron. Lett., 15, 274
 Kleeorin N., Rogachevskii I., Ruzmaikin A. A., 1990, Sov. Phys. JETP, 70, 878
 Kleeorin N., Rogachevskii I., Ruzmaikin A., 1995, A&A, 297, 159
 Kleeorin N., Ruzmaikin A., 1982, Magnetohydrodynamics, 18, 116. Translation from Magnitnaya Gidrodinamika, 2, 17
 Kleeorin N., Ruzmaikin A., 1991, Solar Phys., 131, 211
 Kleeorin Y., Safiullin N., Kleeorin N., Porshnev S., Rogachevskii I., Sokoloff D., 2016, MNRAS, 460, 3960
 Kosovichev A. G., Stenflo J. O., 2008, ApJ Lett., 688, L115
 Krause F., Rädler K.-H., 1980, Mean-Field Magnetohydrodynamics and Dynamo Theory. Pergamon, Oxford
 LaBonte, B. I. & Howard, R.: 1982, Solar Phys., 75, 161
 Leighton, R. B., 1969, ApJ, 156, 1
 Longcope D., Linton M., Pevtsov A., Fisher G., Klapper I., 1999, Twisted flux tubes and how they get that way. In: Magnetic Helicity in Space and Laboratory Plasmas, Geophysical Monograph Series 111, 93
 McClintock B. H., Norton A. A., 2013, Solar Phys. 287, 215
 McClintock B. H., Norton A. A., 2016, ApJ, 818, 7
 McClintock B. H., Norton A. A., Li J., 2014, ApJ, 797, 130
 Moffatt H. K., 1978, Magnetic Field Generation in Electrically Conducting Fluids. Cambridge University Press, New York
 Norton A. A., Gilman P. A., 2005, ApJ, 630, 1194
 Ossendrijver M., 2003, Astron. Astrophys. Rev., 11, 287
 Parker E., 1979, Cosmical Magnetic Fields. Clarendon, Oxford
 Pevtsov A. A., Berger M. A., Nindos A., Norton A. A., van Driel-Gesztelyi L., 2014, Space Sci. Rev. 186, 285
 Pouquet A., Frisch U., Leorat J., 1976, J. Fluid Mech., 77, 321
 Rogachevskii I., Kleeorin N., 2000, Phys. Rev. E, 61, 5202
 Rogachevskii I., Kleeorin N., 2001, Phys. Rev. E., 64, 056307
 Rogachevskii I., Kleeorin N., 2004, Phys. Rev. E, 70, 046310
 Rogachevskii I., Kleeorin N., 2007, Phys. Rev. E, 76, 056307
 Rüdiger G., Hollerbach R., 2004, The Magnetic Universe. Wiley- VCH, Weinheim
 Safiullin N., Kleeorin N., Porshnev S., Rogachevskii I., Ruzmaikin A., 2018, J. Plasma Phys. 84, 735840306
 Sivaraman K. R., Gupta S. S., Howard, R. F., 1999, Solar Phys. 189, 69
 Spruit H. C., 1974, Solar Phys., 34, 277
 Stix M., 1989, The Sun: An Introduction, Springer, Berlin and Heidelberg
 Tlatov A. G., Illarionov E., Sokoloff D., et al., 2013, MNRAS, 432, 2975

- Tlatov A. G., 2015, *Adv. Space Res.*, 55, 851
 Tlatova K., Tlatov A., Pevtsov, A., Mursula, K., Vasileva, V., Heikkinen, E., et al., et al., 2018, *Solar Phys.*, 293, 118
 Tlatova K. A., Vasileva V. V., Pevtsov A. A., 2015, *Geomagn. Aeron.* 55, 896
 Warnecke J., Losada I. R., Brandenburg A., Kleorin N., Rogachevskii I., 2013, *ApJ*, 777, L37
 Warnecke J., Losada I. R., Brandenburg A., Kleorin N., Rogachevskii I., 2016, *A&A*, 589, A125
 Zeldovich Ya. B., Ruzmaikin A. A., Sokoloff, D. D., 1983, *Magnetic Fields in Astrophysics*, Gordon and Breach, New York
 Zhang H., Sokoloff D., Rogachevskii I., Moss D., Lamburt V., Kuzanyan K., Kleorin N., 2006, *MNRAS*, 365, 276
 Zhang H., Moss D., Kleorin N., Kuzanyan K., Rogachevskii I., Sokoloff D., Gao Y., Xu H., *ApJ*, 2012, 751, 47

APPENDIX A: DERIVATION OF EQ. (6) FOR THE MEAN TILT

To derive equation (6) for the mean tilt of sunspot bipolar regions, we exclude the pressure term from equation (5) for ξ by applying **curl** to this equation. This yields

$$\frac{\partial^2 \tilde{\gamma}}{\partial t^2} = 2 \left[\nabla \times \left(\left(\overline{\mathbf{U}} + \frac{\partial \xi}{\partial t} + \mathbf{v}^{(c)} \right) \times \boldsymbol{\Omega} \right) \right] \cdot \mathbf{e}_B + \left(\overline{\mathbf{U}}_A \cdot \nabla \right)^2 \delta_B, \quad (\text{A1})$$

where $\tilde{\gamma} = \boldsymbol{\delta}^{\text{tw}} \cdot \mathbf{e}_B$ is the tilt, $\boldsymbol{\delta}^{\text{tw}} = \nabla \times \xi$ and $\mathbf{e}_B = \overline{\mathbf{B}}/\overline{B}$. We seek for the solution of equation (A1) in the form of standing Alfvén waves as

$$\tilde{\gamma} = \sum_{m=0}^{\infty} A_m \cos \left[\frac{(2m+1)\pi\zeta}{L_B} \right] \cos \left[\frac{2\pi t}{T_m} + \varphi \right], \quad (\text{A2})$$

where $T_m = 2\tau_A/(2m+1)$ is the period of non-dissipating oscillations, $\tau_A = L_B/\overline{U}_A$ is the Alfvén time, ζ is the coordinate along the magnetic field line of the length L_B . Now we take into account that $T_m \Omega \ll 1$, which implies that $|\partial \xi / \partial t| \ll |\mathbf{v}^{(c)}|, |\overline{\mathbf{U}}|$. We also assume that the source of the tilt $I_\gamma = 2 \left[\nabla \times [(\overline{\mathbf{U}} + \mathbf{v}^{(c)}) \times \boldsymbol{\Omega}] \right] \cdot \mathbf{e}_B$ in equation (A1) is localized near the boundary between the solar convective zone and the photosphere. This source can be modelled as the combination of two Dirac delta-functions:

$$I_\gamma(\zeta) = 2 \left[\nabla \times [(\overline{\mathbf{U}} + \mathbf{v}^{(c)}) \times \boldsymbol{\Omega}] \right] \cdot \mathbf{e}_B \times \left[\delta(\zeta/L_B) - \delta(\zeta/L_B - 1) \right], \quad (\text{A3})$$

where $\delta(x)$ is the Dirac delta-function.

We substitute equation (A2) into equation (A1) and after the Fourier transformation of the source term (A3), we obtain equation for the amplitude $A_m(t)$ as

$$\frac{\partial^2 A_m}{\partial t^2} = \frac{2I_\gamma}{\pi} - \left[\overline{U}_A \frac{(2m+1)\pi}{L_B} \right]^2 A_m. \quad (\text{A4})$$

This equation with initial condition $A_m(t=0) = 0$ has the

following solution:

$$A_m(t) = \frac{2I_\gamma \tau_A^2}{\pi^3 (2m+1)^2} \left\{ 1 - \cos \left[\frac{(2m+1)\pi t}{\tau_A} \right] \right\}, \quad (\text{A5})$$

which yields the expression for $\tilde{\gamma}$ as

$$\tilde{\gamma} = \frac{2I_\gamma \tau_A^2}{\pi^3} \sum_{m=0}^{\infty} \frac{1}{(2m+1)^2} \cos \left[\frac{(2m+1)\pi\zeta}{L_B} \right] \times \left\{ 1 - \cos \left[\frac{(2m+1)\pi t}{\tau_A} \right] \right\}. \quad (\text{A6})$$

Averaging equation (A6) over the time that is larger than the maximum Alfvén time τ_A , we obtain equation (6) for the mean tilt $\gamma = \langle \tilde{\gamma} \rangle_{\text{time}}$ of sunspot bipolar regions at the surface of the sun.

APPENDIX B: EQUATION FOR THE RADIAL MEAN VELOCITY

The momentum equation (1) with additional force caused by the eddy viscosity in a steady state in spherical coordinates reads:

$$\frac{\partial}{\partial r} \overline{P}_{\text{tot}} = \frac{2}{r^2} \frac{\partial}{\partial r} \left(r^2 \rho_0 \frac{\overline{U}_r \nu_T}{H_\rho} \right) - \frac{\overline{B}^2}{4\pi r} + 2\rho_0 \overline{U}_\varphi \Omega \sin \theta + \frac{1}{r \sin \theta} \frac{\partial}{\partial \theta} \left(\sin \theta \frac{\rho_0 \overline{U}_\theta \nu_T}{H_\rho} \right), \quad (\text{B1})$$

$$(\text{B2})$$

$$\frac{\partial}{\partial \theta} \overline{P}_{\text{tot}} = \frac{1}{r^2} \frac{\partial}{\partial r} \left(r^3 \rho_0 \frac{\overline{U}_\theta \nu_T}{H_\rho} \right) - \frac{\overline{B}_\varphi^2}{4\pi} \cot \theta + 2\rho_0 \overline{U}_\varphi \Omega r \cos \theta, \quad (\text{B3})$$

Here $\overline{P}_{\text{tot}} = \overline{P} + \overline{B}^2/8\pi + \overline{U}^2/2$ is the total pressure, H_ρ is the density height scale, and ν_T is the eddy viscosity.

We exclude the total pressure term, use the continuity equation $\nabla \cdot (\rho_0 \overline{\mathbf{U}}) = 0$, and introduce the stream function Ψ :

$$\rho_0 \overline{U}_r = \frac{1}{r^2 \sin \theta} \frac{\partial \Psi}{\partial \theta}, \quad \rho_0 \overline{U}_\theta = -\frac{1}{r \sin \theta} \frac{\partial \Psi}{\partial r}. \quad (\text{B4})$$

After neglecting a weak dependence of ν_T/H_ρ on radius r , equations (B1)–(B3) are reduced to

$$\frac{\partial^2 Y}{\partial X^2} + \frac{1}{9X^2} \frac{\partial}{\partial \theta} \left(\frac{1}{\sin \theta} \frac{\partial}{\partial \theta} (Y \sin \theta) \right) = f(X, \theta), \quad (\text{B5})$$

where $X = r^3$, $Y = X \rho_0 \overline{U}_\theta \nu_T / H_\rho$, and

$$f(X, \theta) = \frac{1}{36\pi} \left(\frac{1}{X} \frac{\partial}{\partial \theta} - \frac{3}{\tan \theta} \frac{\partial}{\partial X} \right) \overline{B}_\varphi^2. \quad (\text{B6})$$

Here we take into account that the contribution of the Coriolis force into the function $f(X, \theta)$ under condition of the slow rotation is small (Kleorin & Ruzmaikin 1991; Kleorin et al. 1996). The solution of equation (B5) with the boundary condition

$$\left[(1 - \kappa) \frac{\partial(\rho_0 \overline{U}_r)}{\partial r} + \frac{2\rho_0 \overline{U}_r}{r} \right]_{r=R_\odot} = 0, \quad (\text{B7})$$

is given by

$$\bar{U}_r = \frac{\ell_0^2}{4\pi \kappa \nu_T \rho_{\text{top}} R_\odot} \frac{1}{\sin \theta} \frac{\partial}{\partial \theta} \left[\sin \theta F(\theta) \right]. \quad (\text{B8})$$

where the parameter $\kappa \approx 0.3 - 0.4$ characterises a fraction of the large-scale radial momentum of plasma which is lost during crossing the boundary between the convective zone and photosphere, and

$$F(\theta) \approx \int_{R_\odot - L}^{R_\odot} \left(1 + \frac{R_\odot - r}{L - \ell_0} \right) \left(\frac{\partial \bar{\mathbf{B}}^2}{\partial \theta} \right) \frac{dr}{r} \approx C_u \left(\frac{\partial \bar{\mathbf{B}}^2}{\partial \theta} \right)_{\text{bot}}, \quad (\text{B9})$$

where the constant C_u varies from 0.7 to 1 depending on the radial profile of the mean magnetic field. Therefore, equations (B8)–(B9) yield equation (8).

APPENDIX C: IDENTITIES USED FOR THE DERIVATION OF EQUATION (12)

For the derivation of equation (12) we used identities given below:

$$\sin^3 \phi = \frac{1}{4} [3 \sin \phi - \sin 3\phi], \quad (\text{C1})$$

$$\sin^5 \phi = \frac{1}{16} [10 \sin \phi - 5 \sin 3\phi + \sin 5\phi], \quad (\text{C2})$$

$$\sin^2 \phi \cos \phi = \frac{1}{4} [\cos \phi - \cos 3\phi], \quad (\text{C3})$$

$$\sin^4 \phi \cos \phi = \frac{1}{16} [2 \cos \phi - 3 \cos 3\phi + \cos 5\phi]. \quad (\text{C4})$$

APPENDIX D: THE EVOLUTION OF THE WOLF NUMBER

In the framework of the nonlinear mean-field dynamo model by Kleorin et al. (2016) and Safullin et al. (2018), the phenomenological budget equation for the surface density of the Wolf number is given by

$$\frac{\partial \tilde{W}}{\partial t} = I_w(t, \theta) - \frac{\tilde{W}}{\tau_s(\bar{B})}, \quad (\text{D1})$$

where the rate of production of the surface density of the Wolf number caused by the formation of sunspots is

$$I_w(t, \theta) = \frac{|\gamma_{\text{inst}}| |\bar{B} - \bar{B}_{\text{cr}}|}{\Phi_s} \Theta(\bar{B} - \bar{B}_{\text{cr}}), \quad (\text{D2})$$

and the rate of decay of sunspots is $\tilde{W}/\tau_s(\bar{B})$ with the decay time, $\tau_s(\bar{B})$, of sunspots and $\Theta(x)$ is the Θ function, defined as $\Theta(x) = 1$ for $x > 0$, and $\Theta(x) = 0$ for $x \leq 0$. Here \bar{B}_{cr} is the threshold for the sunspot formation (see below). The phenomenological budget equation (D1) is derived on the idea of negative effective magnetic pressure instability (Kleorin et al. 1989, 1990, 1993, 1996; Kleorin & Rogachevskii 1994) resulting in formation of magnetic spots (Brandenburg et al. 2011, 2013, 2014; Käpylä et al. 2012, 2016) and bipolar active regions

(Warnecke et al. 2013, 2016). The growth rate γ_{inst} of the negative effective magnetic pressure instability is given by

$$\gamma_{\text{inst}} = \left(\frac{2\bar{U}_A^2 k_x^2}{H_\rho^2 k^2} \left| \frac{dP_{\text{eff}}}{d\beta^2} \right| - \frac{4(\boldsymbol{\Omega} \cdot \mathbf{k})^2}{k^2} \right)^{1/2} - \eta_T \left(k^2 + \frac{1}{(2H_\rho)^2} \right), \quad (\text{D3})$$

(Rogachevskii & Kleorin 2007; Brandenburg et al. 2016), where \mathbf{k} is the wave number, $P_{\text{eff}} = \frac{1}{2} [1 - q_p(\beta)] \beta^2$ is the effective magnetic pressure, the nonlinear function $q_p(\beta)$ is the turbulence contribution to the mean magnetic pressure and $\beta = \bar{B}/\bar{B}_{\text{eq}}$. We assume here that the characteristic time of the Wolf number variations is of the order of the characteristic time for excitation of the instability, $\gamma_{\text{inst}}^{-1}$. When the instability is not excited ($\gamma_{\text{inst}} < 0$), the production rate of sunspots, $I_w(t, \theta) \rightarrow 0$, which means that the function $I_w(t, \theta) \propto |\gamma_{\text{inst}}| \Theta(\bar{B} - \bar{B}_{\text{cr}})$. The production term of sunspots is also proportional to the maximum number of sunspots per unit area, which is estimated as $\sim |\bar{B} - \bar{B}_{\text{cr}}|/\Phi_s$, where $|\bar{B} - \bar{B}_{\text{cr}}|$ is the magnetic flux per unit area that contributes to the sunspot formation and Φ_s is the magnetic flux inside a magnetic spot. This instability is excited when the mean magnetic field is larger than a critical value, $\bar{B} > \bar{B}_{\text{cr}}$:

$$\frac{\bar{B}_{\text{cr}}}{\bar{B}_{\text{eq}}} = \frac{\ell_0}{50H_\rho} \left[1 + \left(\frac{10 \text{Co} H_\rho^2}{\ell_0^2} \right)^2 \right]^{1/2}, \quad (\text{D4})$$

This instability is excited in the upper part of the convective zone, where the Coriolis number $\text{Co} = 2\Omega\tau$ is small. The decay time $\tau_s(\bar{B})$ varies from several weeks to a couple of month, while the solar cycle period is about 11 years. This allows us use the steady-state solution of Eq. (D1), $\tilde{W} = \tau_s(\bar{B}) I_w(t, \theta)$. The Wolf number is defined as a surface integral as $W = R_\odot^2 \int \tilde{W}(t, \theta) \sin \theta d\theta d\varphi = 2\pi R_\odot^2 \int \tau_s(\bar{B}) I(t, \theta) \sin \theta d\theta$. The function $\tau_s(\bar{B})$ is given by $\tau_s(\bar{B}) = \tau_* \exp(C_s \partial \bar{B} / \partial t)$, where $C_s = 1.8 \times 10^{-3}$ and $\gamma_{\text{inst}} \tau_* \sim 10$.